

MICROCOMPUTER MODELS FOR HAZARD PREDICTION DOWNSTREAM OF BREACHED DAMS

By D. L. Fread¹

Abstract: Three mathematical models have been developed by the National Weather Service to aid hydrologists/engineers in predicting the downstream flooding due to breached dams. The models (DAMBRK, SMPDBK, BREACH) are available for either microcomputer or mainframe computing systems. The models predict the discharge hydrograph emanating from a breached dam and DAMBRK and SMPDBK route the unsteady flow through the downstream valley thereby determining routed hydrographs, flood arrival times, maximum limits of inundation, and maximum flow velocities at numerous locations along the downstream valley. The models can be used in a real-time hazard warning system or for developing hazard mitigation plans.

Introduction

Catastrophic flooding occurs when a dam fails, and the impounded water escapes through the breach into the downstream valley. Usually, the magnitude of the flow greatly exceeds all previous floods, and warning time is reduced. Three models for predicting the magnitude and timing of the dam-breach flood have been developed by the U.S. National Weather Service. The models (DAMBRK, SMPDBK, BREACH) are coded in Fortran and available at a nominal cost for either microcomputer (IBM PC compatible) or mainframe computing systems.

DAMBRK, developed in 1977, has been adopted for use in the United States by most federal and state agencies concerned with dam safety and design. Also, DAMBRK is being used in several countries within the Americas and elsewhere around the world by governmental agencies, power companies, and private engineering consultants. Research has been on-going in developing improvements in the DAMBRK model allowing it to have an increasing range of application and improved user friendly characteristics. The model can be used as part of a real-time hazard warning system or for developing hazard mitigation plans. Also, DAMBRK can be used for routing any specified hydrograph through reservoirs, rivers, canals, or estuaries as part of general engineering studies of waterways. Recently, DAMBRK has been expanded to route mud/debris flow hydrographs. SMPDBK, developed in 1982-83, is a much simplified technique for predicting dam-breach flooding. It has received considerable use in the United States when available time and resources are too limited for the use of DAMBRK and the attendant reduction in accuracy is judged acceptable. BREACH, developed in 1984-85, predicts only the breach hydrograph and the breach size and its time of formation due to overtopping or piping of earthen/rockfill dams. It has thus far received rather limited application for selecting the breach parameters required by DAMBRK and SMPDBK. BREACH should be used with judgment and caution until it receives further verification to determine its extent of applicability and reliability.

This paper presents a brief description of each model, an application of each, and comments concerning on-going research and development.

DAMBRK

The DAMBRK model (4, 5, 7) represents the current state-of-the-art in understanding dam failures and the utilization of hydrodynamic theory to predict the dam-break wave formation and downstream progression. The model

¹Sr. Research Hydrologist, Hydrologic Res. Lab., Office of Hydrology, National Weather Service, NOAA, Silver Spring, MD 20910.

has wide applicability; it can function with various levels of input data ranging from rough estimates to complete data specification; the required data is readily accessible; and it is economically feasible to use, i.e., it requires minimal computational effort on mainframe computing facilities and can be used with microcomputers. DAMBRK is used to develop the outflow hydrograph from a dam and hydraulically route the flood through the downstream valley. The governing equations of the model are the complete one-dimensional Saint-Venant equations of unsteady flow which are coupled with internal boundary equations representing the rapidly varied flow through structures such as dams and bridge/embankments which may develop a time-dependent breach. Also, appropriate external boundary equations at the upstream and downstream ends of the routing reach are utilized. The system of equations is solved by a nonlinear weighted 4-point implicit finite difference method. The flow may be either subcritical or supercritical with fluid properties obeying either Newtonian or non-Newtonian plastic principles. The hydrograph to be routed may be specified as an input time series or it can be developed by the model using specified breach parameters (size, shape, time of development). The possible presence of downstream dams which may be breached by the flood, bridge/embankment flow constrictions, tributary inflows, river sinuosity, levees located along the downstream river, and tidal effects are each properly considered during the downstream propagation of the flood. DAMBRK also may be used to route mud and debris flows or rainfall/snowmelt floods using specified upstream hydrographs. High water profiles along the valley, flood arrival times, and hydrographs at user selected locations are standard model output.

Saint-Venant Equations.--A modified and expanded form of the original Saint-Venant equations (2,7) consist of a conservation of mass equation, i.e.,

$$\frac{\partial Q}{\partial x} + \frac{\partial s(A+A_o)}{\partial t} - q = 0 \quad \dots\dots\dots (1)$$

and a conservation of momentum equation, i.e.,

$$\frac{\partial(sQ)}{\partial t} + \frac{\partial(Q^2/A)}{\partial x} + gA\left(\frac{\partial h}{\partial x} + S_f + S_e + S_i\right) + L = 0 \quad \dots\dots\dots (2)$$

where h is the water surface elevation, A is the active cross-sectional area of flow, A_o is the inactive (off-channel storage) cross-sectional area, s is a sinuosity factor (2) which varies with h, x is the longitudinal distance along the channel (valley), t is the time, q is the lateral inflow or outflow per linear distance along the channel (inflow is positive and outflow is negative in sign), g is the acceleration due to gravity, S_f is the boundary friction slope, and S_e is the expansion-contraction slope, and S_i is the additional friction slope associated with internal viscous dissipation of non-Newtonian fluids such as mud/debris flows. The boundary friction slope is evaluated from Manning's equation for uniform, steady flow, i.e.,

$$S_f = \frac{n^2 |Q|Q}{2.21 A^2 R^{4/3}} = |Q|Q/K^2 \quad \dots\dots\dots (3)$$

in which n is the Manning coefficient of frictional resistance, R is the hydraulic radius, and K is the channel conveyance factor. The term (S_e) is

$$S_e = \frac{k \Delta(Q/A)^2}{2g \Delta x} \quad \dots\dots\dots (4)$$

in which k is the expansion-contraction coefficient varying from 0.0 to ±1.0 (+ if contraction, - if expansion), and Δ(Q/A)² is the difference in the term (Q/A)² at two adjacent cross-sections separated by a distance Δx. L is the

momentum effect of lateral flow assumed herein to enter or exit perpendicular to the direction of the main flow. This term has the following form: 1) lateral inflow, $L = 0$; 2) seepage lateral outflow, $L = -0.5qQ/A$; and 3) bulk lateral outflow, $L = -qQ/A$. The term (S_1) can be significant only when the fluid is non-Newtonian. It is evaluated for any non-Newtonian flow as follows:

$$S_1 = \frac{\kappa}{\gamma} \left[\frac{(b+2)Q}{AD^{b+1}} + \frac{(b+2)(\tau_0/\kappa)^b}{2D^b} \right]^{1/b} \dots\dots\dots (5)$$

in which γ is the fluid's unit weight, τ_0 is the fluid's yield strength, D is the hydraulic depth (ratio of wetted area to top width), $b=1/m$ where m is the power of the power function that fits the fluid's stress-strain properties, and κ is the the apparent viscosity or scale factor of the power function.

Eqs. 1 and 2, which are nonlinear partial differential equations, must be solved by numerical techniques. An implicit 4-point finite difference technique is used to obtain the solution. This particular technique is used for its computational efficiency, flexibility, and convenience in the application of the equations to flow in complex channels existing in nature. In essence, the technique determines the unknown quantities (Q and h at all specified cross-sections along the downstream channel-valley) at various times into the future; the solution is advanced from one time to a future time by a finite time interval (time step) of magnitude Δt . The flow equations are expressed in finite difference form for all cross-sections along the valley and then solved simultaneously for the unknowns (Q and h) at each cross-section. Due to the nonlinearity of the partial differential equations and their finite difference representations, the solution is iterative and a highly efficient quadratic iterative technique known as the Newton-Raphson method is used. Convergence of the iterative technique is attained when the difference between successive iterative solutions for each unknown is less than a relatively small prescribed tolerance. Usually, one to three iterations at each time step are sufficient for convergence to be attained for each unknown at all cross-sections. A more complete description of the solution technique may be found elsewhere (7).

Internal Boundaries.--A dam is considered an internal boundary which is defined as a short Δx reach between sections i and $i+1$ in which the flow is governed by the following two equations rather than Eqs. 1 and 2:

$$Q_i = Q_{i+1} \dots\dots\dots (6)$$

$$Q_i = Q_s + Q_b \dots\dots\dots (7)$$

in which Q_s and Q_b are the spillway and breach flow, respectively. In this way, the flows Q_i and Q_{i+1} and the elevations h_i and h_{i+1} are in balance with the other flows and elevations occurring simultaneously throughout the entire flow system which may consist of additional dams which are treated as additional internal boundary conditions via Eqs. 6 and 7. In fact, DAMBRK can simulate the progression of a dam-break flood through an unlimited number of reservoirs located sequentially along the valley. The downstream dams may also breach if they are sufficiently overtopped. The spillway flow (Q_s) is computed from the following expression:

$$Q_s = c_s L_s (h-h_s)^{1.5} + c_g A_g (h-h_g)^{0.5} + c_d L_d (h-h_d)^{1.5} + Q_t \dots\dots\dots (8)$$

in which c_s is the uncontrolled spillway discharge coefficient, h_s is the uncontrolled spillway crest, c_g is the gated spillway discharge coefficient, h_g is the center-line elevation of the gated spillway, c_d is the discharge coefficient for flow over the crest of the dam, L_s is the spillway length, A_g is the gate flow area, L_d is the length of the dam crest less L_s , and Q_t is a constant outflow term which is head independent. The uncontrolled spillway flow or the gated spillway flow can also be represented as a table of head-discharge values. The gate flow may also be specified as a function of time. The breach outflow (Q_s) is computed as broad-crested weir flow, i.e.,

$$Q_b = c_v k_s [3.1 b_i (h - h_b)^{1.5} + 2.45 z (h - h_b)^{2.5}] \dots\dots\dots (9)$$

in which c_v is a small correction for velocity of approach, b_i is the instantaneous breach bottom width, h is the elevation of the water surface just upstream of the structure, h_b is the elevation of the breach bottom which is assumed to be a linear function of the breach formation time, z is the side slope of the breach, and k_s is the submergence correction due to downstream tailwater elevation (h_t), i.e.,

$$k_s = 1.0 - 27.8 \left[\frac{h_t - h_b}{h - h_b} - 0.67 \right]^3 \dots\dots\dots (10)$$

If the breach is formed by piping, Eq. 9 is replaced by an orifice equation:

$$Q_b = 4.8 A_p (h - h_f)^{1/2} \dots\dots\dots (11)$$

$$\text{where: } A_p = [2b_i + 4z(h_f - h_b)] (h_f - h_b) \dots\dots\dots (12)$$

in which h_f is the specified center-line elevation of the pipe.

Highway/railway bridges and their associated earthen embankments which are located at points downstream of a dam may also be treated as internal boundary conditions. Eqs. 6 and 7 are used at each bridge; the term Q_s in Eq. 7 is computed by the following expression:

$$Q_s = C\sqrt{2g} A_{i+1} (h_i - h_{i+1})^{0.5} + C_d k_s (h - h_c)^{1.5} \dots\dots\dots (13)$$

in which C is a coefficient of bridge flow, C_d is the coefficient of flow over the crest of the road embankment, h_c is the crest elevation of the embankment, and k_s is similar to Eq. 10. A breach of the embankment is treated the same as with dams.

Breach.--The breach is the opening formed in the dam as it fails. Earthen dams which exceedingly outnumber all other types of dams do not tend to completely fail, nor do they fail instantaneously. The fully formed breach in earthen dams tends to have an average width (\bar{b}) in the range ($h_d < \bar{b} < \frac{4}{3}h_d$) where h_d is the height of the dam. The middle portion of this range for \bar{b} is supported by the summary report of Johnson and Illes (8). Breach widths for earthen dams are therefore usually much less than the total length of the dam as measured across the valley. Also, the breach requires a finite interval of time (τ) for its formation through erosion of the dam materials by the escaping water. Total time of failure may be in the range of a few minutes to a few hours, depending on the height of the dam, the type of materials used in construction, the extent of compaction of the materials, and the magnitude and duration of the overtopping flow of the escaping water. Piping failures occur when initial breach formation takes place at some point below the top of the dam due to erosion of an internal channel through the dam by escaping water.

As the erosion proceeds, a larger and larger opening is formed; this is eventually hastened by caving-in of the top portion of the dam. Concrete gravity dams also tend to have a partial breach as one or more monolith sections formed during the construction of the dam are forced apart by the escaping water. The time for breach formation is in the range of a few minutes. Poorly constructed earthen dams and coal-waste slag piles which impound water tend to fail within a few minutes, and have average breach widths in the upper range or even greater than those for the earthen dams mentioned above.

In DAMBRK, the failure time (τ) and the size and shape of the breach are selected as input parameters similar to the approach used by Fread and Harbaugh (3). The shape is specified by a parameter (z) identifying the side slope of the breach, i.e., 1 vertical: z horizontal. Rectangular, triangular, or trapezoidal shapes may be specified in this way. For example, $z > 0$ and $b > 0$ produces a trapezoidal shape. The final breach size is controlled by the z parameter and another parameter (b) which is the terminal width of the bottom of the breach. The model assumes the breach bottom width starts at a point and enlarges at a linear rate over the failure time (τ) until the terminal width is attained and the breach bottom has eroded to the elevation h_{bm} which is usually, but not necessarily, the bottom of the reservoir or outlet channel bottom. During the simulation of a dam failure, the actual breach formation commences when the reservoir water surface elevation (h) exceeds a specified value, h_f . This feature permits the simulation of an overtopping of a dam in which the breach does not form until a sufficient amount of water is flowing over the crest of the dam. A piping failure is simulated when h_f is specified less than the height of the dam, h_d .

External Boundaries.--The upstream boundary (a known relationship between flow and depth or time) is usually $Q = QI(t)$. If the water surface of the most upstream reservoir is assumed to remain level as it varies with time, then the following boundary equation is used:

$$Q_1 = QI(t) - 0.5 \bar{S}_a 43560. \Delta h / \Delta t \dots\dots\dots (14)$$

in which Q_1 is the discharge at the upstream most section (the upstream face of the dam), $QI(t)$ is the specified inflow to the reservoir, \bar{S}_a is the average surface area (acre-ft) of the reservoir during the Δt time interval, and Δh is the change in reservoir elevation during the time step. If the flow is supercritical throughout the routing reach, two boundary equations are used at the upstream section, i.e., $Q_1 = QI(t)$ and $Q_1 = KS^{0.5}$ in which K is the channel conveyance and S is the instantaneous water surface slope.

For subcritical flows, a known relationship between flow and depth or time must be specified for the most downstream section. The downstream boundary is often a rating table of discharge associated with a particular depth. It may also be a known water elevation variation with time such as a large tidal bay or lake. If the flow is supercritical, no downstream boundary is required since downstream flow disturbances do not progress upstream.

Lateral flows.--Unsteady flows associated with tributaries upstream or downstream of a dam can be added to the unsteady flow resulting from the dam failure. This is accomplished via the term q in Eq. 1. The tributary flow is distributed along a single Δx reach. Backwater effects of the dam-break flow on the tributary flow are ignored, and the tributary flow is assumed to enter perpendicular to the dam-break flow. Outflows are assigned negative values. Outflows which occur as broad-crested weir flow over a levee or natural crest may be simulated. The crest elevation, discharge coefficient, and location

along the river-valley must be specified. The head is computed as the average water surface elevation, along the crest length, less the crest elevation.

Floodplain Compartments.--The DAMBRK model can simulate the exchange of flow between the river and floodplain compartments. The floodplain compartments are formed by one or two levees which run parallel to the river on either or both sides of the river, and other levees or road embankments which run perpendicular to the river. Flow transfer between a floodplain compartment and the river is assumed to occur along one Δx reach and is controlled by broad-crested weir flow with submergence correction. Flow can be either away from the river or into the river, depending on the relative water surface elevations of the river and the floodplain compartment. The river elevations are computed via Eqs. 1 and 2, and the floodplain water surface elevations are computed by a simple storage routing relation, i.e.,

$$V_L^t = V_L^{t-\Delta t} + (I^t - O^t) \Delta t / 43560 \dots\dots\dots (15)$$

in which V_L is the volume (acre-ft) in the floodplain compartment at time t or $t-\Delta t$ referenced to the water elevation, I is the inflow from the river or adjacent floodplain compartments, and O is the outflow from the floodplain compartment to the river and/or to adjacent floodplain compartments. Flow transfer between adjacent floodplain compartments is controlled by broad-crested weir flow with submergence correction. The outflow from a floodplain compartment may also include that from one or more pumps associated with each floodplain compartment. Each pump has a specified discharge-head relation given in tabular form along with specified start-up and shut-off operating elevations. The pumps discharge to the river.

Landslide Waves.--The capability to generate a wave produced by a landslide, which rushes into a reservoir, is provided within DAMBRK. The volume of the landslide mass, its porosity, and time interval over which the landslide occurs, are input to the model. Within the model, the landslide mass is deposited within the reservoir in layers during small computational time steps, and simultaneously the original dimensions of the reservoir are reduced accordingly. The time rate of reduction in the reservoir cross-sectional area creates the wave during the solution of the unsteady flow Eqs. 1 and 2, applied to the cross-sections describing the reservoir characteristics. The wave may have sufficient amplitude to overtop the dam and precipitate a failure of the dam, or the wave by itself may be large enough to cause catastrophic flooding downstream of the dam without resulting in the failure of the dam as perhaps in the case of a concrete dam.

Model Testing.--The DAMBRK model has been tested on several historical floods due to breached dams to determine its ability to reconstitute observed downstream peak stages, discharges, and travel times. Among the floods that have been used in the testing are: 1976 Teton Dam, 1972 Buffalo Creek Coal-Waste Dam, 1889 Johnstown Dam, 1977 Toccoa (Kelly Barnes) Dam, and the 1977 Laurel Run Dam floods. However, only the Teton and Buffalo Creek peak flow profiles are presented herein.

The Teton Dam, a 300 ft (91.4 m) high earthen dam with 230,000 acre-ft (282,900,000 m^3) of stored water and maximum 262.5 ft (80 m) water depth, failed on June 5, 1976, killing 11 people making 25,000 homeless, and inflicting about \$400 million in damages to the downstream Teton-Snake River Valley. Data from a Geological Survey Report (9) provided observations on the approximate development of the breach, description of the reservoir storage, downstream cross-sections and estimates of Manning's n approximately every 5 miles, estimated peak discharge measurements at four sites, flood peak travel

times, and flood peak elevations. The critical breach parameters were $\tau = 0.85$ hrs, $b = 80$ ft (24.4 m), and $z = 0.7$. The computed peak flow profile along the downstream valley is shown in Fig. 1. Variations between computed and observed values are less than 5 percent.

The Buffalo Creek "coal waste" dam, a 44 ft (13.4 m) high tailings dam with 400 acre-ft (492,000 m³) of storage failed on February 26, 1972, resulting in 118 lives lost and over \$50 million in property damage. Flood observations (1) along with the computed flood peak profile extending about 16 miles downstream are shown in Fig. 2. Critical breach parameters were $\tau = 0.08$ hrs, $b = 170$ ft (49.2 m), and $z = 2.6$. Comparison of computed and observed flows indicate an average difference of about 9 percent.

Current Research.--Research and development efforts concerning the DAMBRK model include the following: (a) simulation of flows which change with time and location between subcritical and supercritical regimes (7); (b) improving the numerical robustness of the 4-pt implicit solution via proper distance step selection, use of channel conveyance rather than the Manning equation, and smoothing of the initial rise of the dam-breach hydrograph; (c) determining the degree of nonlinearity as a breach parameter; (d) development of interactive user-friendly data input; and (e) development of synthesis technique for mud/debris flow hydrographs.

SMPDBK

The SMPDBK model, as described in detail by Wetmore and Fread (11), is a simple model for predicting the characteristics of the floodwave peak produced by a breached dam. It will, with minimal computational resources (hand-held calculators, microcomputers), determine the peak flow, depth, and time of occurrence at selected locations downstream of a breached dam. SMPDBK first computes the peak outflow at the dam, based on the reservoir size and the temporal and geometrical description of the breach. The computed floodwave and channel properties are used in conjunction with routing curves to determine how the peak flow will be diminished as it moves downstream. Based on this predicted floodwave reduction, the model computes the peak flows at specified downstream points. The model then computes the depth reached by the peak flow based on the channel geometry, slope, and roughness at these downstream points. The model also computes the time required for the peak to reach each forecast point and, if a flood depth is entered for the point, the time at which that depth is reached as well as when the floodwave recedes below that depth, thus providing a time frame for evacuation and fortification on which a preparedness plan may be based. The SMPDBK model neglects backwater effects created by downstream dams or bridge embankments, the presence of which can substantially reduce the model's accuracy. However, its speed and ease of use together with its small computational requirements make it an attractive tool for use in cases where limited time and resources preclude the use of the DAMBRK model. In such instances planners, designers, emergency managers, and consulting engineers responsible for predicting the potential effects of a dam failure may employ the model where backwater effects are not significant.

The SMPDBK model retains the critical deterministic components of the DAMBRK model while eliminating the need for extensive numerical computations. It accomplishes this by approximating the downstream channel/valley as a prism, concerning itself with only the peak flows, stages, and travel times, neglecting the effects of backwater from downstream bridges and dams, and utilizing dimensionless peak-flow routing graphs developed by using the DAMBRK model. The applicability of the SMPDBK model is enhanced with its user friendly interactive input and option for minimal data requirements. The peak flow at the dam may be computed with only four readily accessible data values

and the downstream channel/valley may be defined with a single average cross section, although prediction accuracy increases with the number of specified cross sections.

Breach Outflow.--The model uses a single equation to determine the maximum breach outflow and the user is required to supply the values of four variables for this equation. These variables are: 1) the surface area (A_s , acres) of the reservoir; 2) the depth (H , ft) to which the breach cuts; 3) the time (t_f , minutes) required for breach formation; and 4) the final width (B_r , ft) of the breach. These parameters are substituted into a broad-crested weir flow equation to yield the maximum breach outflow (Q_{bmax}) in cfs, i.e.,

$$Q_{bmax} = Q_o + 3.1 B_r \left(\frac{C}{t_f/60 + C/\sqrt{H}} \right)^3 \dots\dots\dots (16)$$

$$\text{where: } C = \frac{23.4 A_s}{B_r} \dots\dots\dots (17)$$

and Q_o is the spillway flow and overtopping crest flow which is estimated to occur simultaneously with the peak breach outflow.

Once the maximum outflow at the dam has been computed, the depth of flow produced by this discharge may be determined based on the geometry of the channel immediately downstream of the dam, the Manning "n" (roughness coefficient) of the channel and the slope of the downstream channel. This depth is then compared to the depth of water in the reservoir to find whether it is necessary to include a submergence correction factor for tailwater effects on the breach outflow, i.e., to determine if the water downstream is restricting the free flow through the breach. This comparison and (if necessary) correction allows the model to provide the most accurate prediction of maximum breach outflow which properly accounts for the effects of tailwater depth downstream of the dam. The submergence correction is computed from Eq. 10 and must be applied iteratively since the outflow produces the tailwater depth which determines the submergence factor which affects the outflow.

Peak Flow Routing.--The peak discharge is routed to downstream points of interest through the channel/valley described by selected cross sections defined by tables of widths and associated elevations. The routing reach from the dam to the point of interest is approximated as a prismatic channel by defining a single cross section (an average section that incorporates the geometric properties of all intervening sections via a distance weighting technique). This prismatic representation of the channel allows easy calculation of flow area and volume in the downstream channel which is required to accurately predict the amount of peak flow attenuation. The peak flow at the dam computed from Eq. 16 is routed downstream using the dimensionless routing curves (see Fig. 3). These curves were developed from numerous executions of the NWS DAMBRK model and they are grouped into families based on the Froude number associated with the floodwave peak, and have as their X-coordinate the ratio of the downstream distance (from the dam to a selected cross section) to a distance parameter (X_c). The Y-coordinate of the curves used in predicting peak downstream flows is the ratio of the peak flow at the selected cross section to the computed peak flow at the dam. The distinguishing characteristic of each member of a family is the ratio (V^*) of the volume in the reservoir to the average flow volume in the downstream channel. Thus it may be seen that to predict the peak flow of the floodwave at a downstream point, the desired distinguishing characteristic of the curve family and member must be determined. This determination is based on the calculation of the Froude number

(F_c) and the volume ratio parameter (V^*). To specify the distance in dimensionless form, the distance parameter (X_c) in ft is computed as follows:

$$X_c = 6 \text{ VOL} / [\bar{A}(1 + 4(0.5)^{m+1})] \dots\dots\dots (18)$$

in which VOL is the reservoir volume (acre-ft), m is a shape factor for the prismatic routing reach, and \bar{A} is the average cross-section area in the routing reach at a depth corresponding to the height of the dam. The volume parameter (V^*) is simply $V^* = \text{VOL} / (\bar{A}_c X_c)$ in which \bar{A}_c represents the average cross-sectional area in the routing reach at the average maximum depth produced by the routed flow. The Froude Number (F_c) is simply $F_c = V_c / (g D_c)^{0.5}$ where V_c and D_c are the average velocity and hydraulic depth, respectively, within the routing reach. Further details on the computation of the dimensionless parameters can be found elsewhere (11). Using families of curves similar to Fig. 3, the routed peak discharge can be obtained. The corresponding peak depth is computed from the Manning equation using an iterative method since the wetted area and hydraulic radius are nonlinear functions of the unknown depth.

The time of occurrence of the peak flow at a selected cross section is determined by adding the time of failure to the peak travel time from the dam to that cross section. The travel time is computed using the kinematic wave velocity which is a known function of the average flow velocity throughout the routing reach. The times of first flooding and "de-flooding" of a particular elevation at the cross section may also be determined within SMPDBK. Further description of the computational procedure for determining these times, as well as, the time of peak flow may be found elsewhere (11).

Testing and Verification.--The SMPDBK model was compared with the DAMBRK model in several theoretical applications where backwater effects were negligible. The average difference between the two models was 10-20 percent for predicted flows and travel times with depth differences of less than about 1 ft (0.3 m). Since the DAMBRK model is considered more accurate, the differences can be considered errors due to the simplifications of SMPDBK. The application of SMPDBK to the Teton dam breach is shown in Fig. 1, and its application to the Buffalo Creek "coal waste" dam breach is shown in Fig. 2. In each case, the peak discharge profile computed with DAMBRK, and the observed peak flows are shown for comparison. On-going research and development concerning the SMPDBK model has resulted in the following improvements: (a) the interactive data input has been considerably improved allowing real-time editing capabilities and creation of a permanent data file; (b) an option to use an existing "batch" input file; (c) peak depths are computed using the original cross-section properties entered as width-elevation tables rather than using a fitted "power function" curve to replace the table (this eliminates possible significant fitting errors); (d) extension of the routing curves for Froude numbers above 0.75 by using a nonlinear extrapolation procedure. Current research is directed at possibly including the effects of downstream bridge constrictions.

BREACH

This model (6) predicts the outflow hydrograph from a breached dam and the breach size, shape, and time of formation of a breach in earthen/rockfill dams where the breach may be initiated by either piping or overtopping. The dam can be man-made with either homogeneous fill or fill with a distinctive central core. The downstream face may be grass covered or bare. The model utilizes the principles of soil mechanics, hydraulics, and sediment transport to simulate the erosion and bank collapse processes which form the breach. Reservoir inflow, storage, and spillway characteristics, along with the geo-

metrical and material properties of the dam (D_{50} , size, cohesion, internal friction angle, porosity, and unit weight) are utilized to predict the outflow hydrograph. The essential model components are described as follows.

Reservoir Level Computation.--Conservation of mass is used to compute the reservoir water surface elevation (H) due to the influence of a specified reservoir inflow hydrograph (Q_i), spillway overflow (Q_{sp}) as determined from a spillway rating table, broad-crested weir flow (Q_o) over the crest of the dam, broad-crested weir flow (Q_b) through the breach, and the reservoir storage characteristics described by a surface area (S_a)-elevation table. Letting ΔH represent the change in reservoir level during a small time interval (Δt), the conservation of mass requires the following relationship:

$$\Delta H = \frac{0.0826 \Delta t}{S_a} (\bar{Q}_i - \bar{Q}_b - \bar{Q}_{sp} - \bar{Q}_o) \dots\dots\dots (19)$$

in which the bar (-) denotes the average value during the Δt time interval. Thus, the reservoir elevation (H) at time (t) can easily be obtained since, $H = H' + \Delta H$, in which H' is the reservoir elevation at time ($t - \Delta t$). If the breach is formed by piping, a short-tube, orifice flow equation is used instead of a broad-crested weir flow equation, i.e.,

$$Q_b = 3 A_b (H - h_b)^{0.5} \quad (\text{broad-crested weir flow}) \dots\dots\dots (20)$$

$$Q_b = A_b [2g(H-h_p)/(1 + fL/D)]^{0.5} \quad (\text{orifice flow}) \dots\dots\dots (21)$$

in which A_b is the area of flow over the weir or orifice area, h_b is the elevation of the bottom of the breach at the upstream face of the dam, h_p is the specified center-line elevation of the pipe, f is the Darcy friction factor which is dependent on the D_{50} grain size, L is the length of the pipe, and D is the diameter or width of the pipe.

Breach Width.--Initially the breach is considered rectangular with the width (B_o) based on the assumption of optimal channel hydraulic efficiency, $B_o = B_r Y$ in which Y is the critical depth of flow at the entrance to the breach; i.e., $Y = 2/3(H-h_b)$. The factor B_r is set to 2 for overtopping and 1 for piping. The initial rectangular-shaped breach can change to a trapezoidal shape when the sides of the breach collapse due to the breach depth exceeding the limits of a free-standing cut in soil of specified properties of cohesion (C), internal friction angel (ϕ), unit weight (γ) and existing angle (θ') that the breach cut makes with the horizontal. The collapse occurs when the effective breach depth (d') exceeds the critical depth (d_c), i.e.,

$$d_c = 4C \cos \phi \sin \theta' / [\gamma - \gamma \cos(\theta' - \phi)] \dots\dots\dots (22)$$

The effective breach depth (d') is determined by reducing the actual breach depth (d) by $Y/3$ to account for the supporting influence of the water flowing through the breach. The θ' angle reduces to a new angle upon collapse which is simply $\theta = (\theta' + \phi)/2$. The model allows up to three collapses to occur.

Breach Erosion.--Erosion is assumed to occur equally along the bottom and sides of the breach except when the sides of the breach collapse. Then, the breach bottom is assumed not to continue to erode downward until the volume of collapsed material along the length of the breach is removed at the rate of sediment transport occurring along the breach at the instant before collapse. After this characteristically short pause, the breach bottom and sides continue to erode. Material above the wetted portion of the eroding breach sides is assumed to simultaneously collapse as the sides erode. Once the

breach has eroded to the specified bottom of the dam, erosion continues to occur only along the sides of the breach. The rate at which the breach is eroded depends on the capacity of the flowing water to transport the eroded material. The Meyer-Peter and Muller sediment transport relation as modified by Smart (10) for steep channels is used, i.e.,

$$Q_s = 3.64 (D_{90}/D_{30})^{0.2} \frac{D^{2/3}}{n} S^{1.1} (DS - 0.0054 D_{50} \tau_c) \dots\dots\dots (23)$$

in which Q_s is the sediment transport rate, D_{90} , D_{30} , D_{50} are the grain sizes in (mm) at which 90, 30, and 50 percent respectively of the total weight is finer, D is the hydraulic depth of flow computed from Manning's equation for flow along the breach at any instant of time, S is the breach bottom slope which is assumed to always be parallel to the downstream face of the dam, and τ_c is Shield's critical shear stress that must be exceeded before erosion occurs. The incremental increase in the breach bottom and sides (ΔH_c) which occurs over a very short interval of time is given by:

$$\Delta H_c = Q_s \Delta t / [P L (1-p)] \dots\dots\dots (24)$$

in which P is the total perimeter of the breach, L is the length of the breach through the dam, and p is the porosity of the breach material.

Computational Algorithm.--The sequence of computations in the model are iterative since the flow into the breach is dependent on the bottom elevation of the breach and its width while the breach dimensions are dependent on the sediment transport capacity of the breach flow; and the sediment transport capacity is dependent on the breach size and flow. A simple iterative algorithm is used to account for the mutual dependence of the flow, erosion, and breach properties. An estimated incremental erosion depth ($\Delta H'_c$) is used at each time step to start the iterative solution. This estimated value can be extrapolated from previously computed values. Convergence is assumed when ΔH_c computed from Eq. 24 differs from $\Delta H'_c$ by an acceptable specified tolerance. Typical applications of the breach model require less than 2 minutes on microcomputers with a fast arithmetic processor. The computations show very little sensitivity to a reasonable variation in the specified time step size. The model has displayed a lack of numerical instability or convergence problems.

Teton Application.--BREACH was applied to the piping initiated failure of the Teton earthfill dam which breached in June 1976, releasing an estimated peak discharge of 2.3 million cfs (65,128 cms) having a range of 1.6 to 2.6 million cfs. The simulated breach hydrograph is shown in Fig. 4. The computed final top breach width of the trapezoidal breach was 645 ft (213 m) compared to the observed width of 650 ft (214.7 m). The computed side slope of the breach was 1:1.06 compared to 1:1.00. Additional information on this and another application of BREACH to the naturally formed landslide dam on the Mantaro River in Peru, which breached in June 1974, can be found elsewhere (6). The model has also been satisfactorily verified with the piping initiated failure of the 28 ft (8.5 m) high Lawn Lake dam in Colorado in 1982. BREACH will continue to be tested as data becomes available.

Summary

Three NWS models for predicting the flooding due to dam failures are summarized. The BREACH model can aid the hydrologist/engineer in determining the properties of the piping or overtopping initiated breach of an earthen dam. This information can be used in conjunction with historical breach data to create the dam breach hydrograph and route it through the downstream channel-

valley using the complex DAMBRK model or the simplified SMPDBK model. The choice of either the DAMBRK or SMPDBK model is influenced by the available time, data, computer facilities, modeling experience, and required accuracy for each dam break analysis. Complexities in the downstream channel valley such as highway/railway embankment-bridges, significant channel constrictions, levee overtopping, flow volume losses, downstream dams, weirs, and lakes require the DAMBRK model to be used rather than the SMPDBK model since the latter model ignores such factors.

Appendix I.-- References

1. Davies, W. E., Baily, J. F., and Kelly, D. B., "West Virginia's Buffalo Creek Flood: A Study of the Hydrology and Engineering Geology," Geological Survey, Circular 667, U.S. Geological Survey, 1975, 32 pp.
2. DeLong, L. L., "Extension of the Unsteady One-Dimensional Open Channel Flow Equations for Flow Simulation in Meandering Channels with Flood Plains," Selected Papers in HydroScience, 1985, pp. 101-105.
3. Fread, D. L., and Harbaugh, T. E., "Transient Hydraulic Simulation of Breached Earth Dams," Journal of the Hydraulics Division, American Society of Civil Engineers, Vol. 99, No. HY1, Jan., 1973, pp. 139-154.
4. Fread, D. L., "The Development and Testing of a Dam-Break Flood Forecasting Model," Proceedings, Dam-Break Flood Modeling Workshop, U.S. Water Resources Council, Oct. 18-20, 1977, Washington, D.C., 32 pp.
5. Fread, D. L., "DAMBRK: The NWS Dam-Break Flood Forecasting Model," Hydrologic Research Laboratory, National Weather Service, Silver Spring, MD, 1984, 56 pp.
6. Fread, D. L., "A Breach Erosion Model for Earthen Dams," Proceedings of Specialty Conference on Delineation of Landslides, Flash Flood, and Debris Flow Hazards in Utah, Utah State University, June 15, 1984, 30 pp.
7. Fread, D. L., "Channel Routing," Hydrological Forecasting, (Editors: M. G. Anderson and T. P. Burt), Chapter 14, John Wiley and Sons, 1985, pp. 437-503.
8. Johnson, F. A., and Illes, P., "A Classification of Dam Failures," Water Power and Dam Construction, Dec., 1976, pp. 43-45.
9. Ray, H. A., Kjelstrom, L.C., Crosthwaite, E. G., and Low, W. H., "The Flood in Southeastern Idaho from Teton Dam Failure of June 5, 1976," Open File Report, U.S. Geological Survey, Boise, ID, 1976.
10. Smart, G. M., "Sediment Transport Formula for Steep Channels," Journal of Hydraulics Division, American Society of Civil Engineers, Vol. 110, No. 3, 1984, pp. 267-276.
11. Wetmore, J. N., and Fread, D. L., "The NWS Simplified Dam Break Flood Forecasting Model," printed and distributed by the Federal Emergency Management Agency (FEMA), 1984, 122 pp.

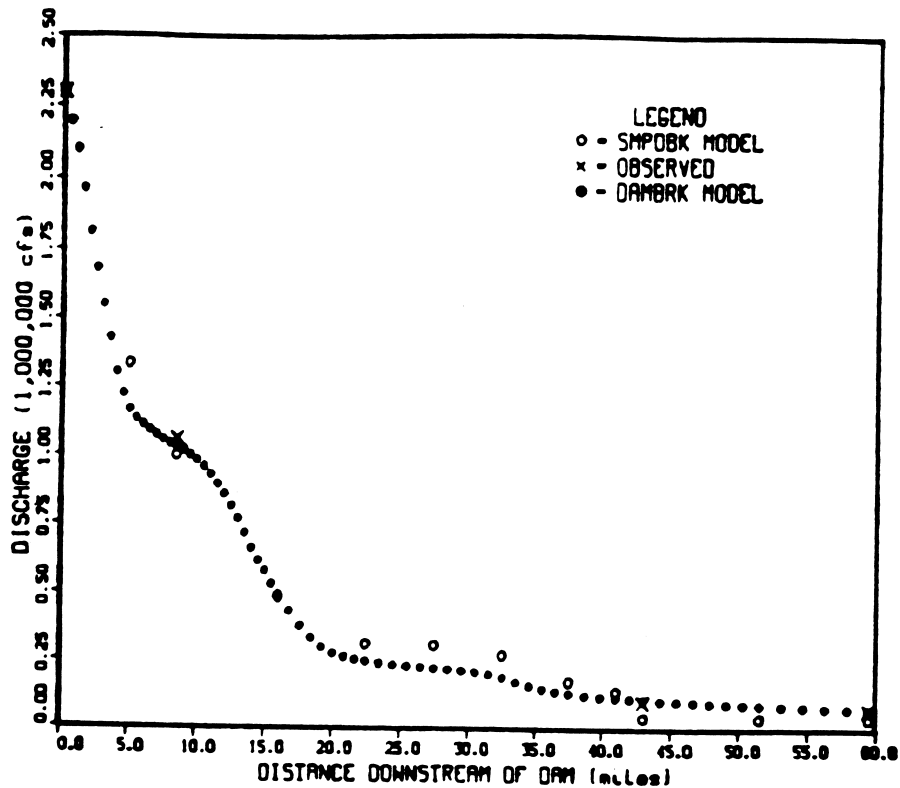


FIG. 1 PROFILE OF PEAK DISCHARGE DOWNSTREAM OF TETON.

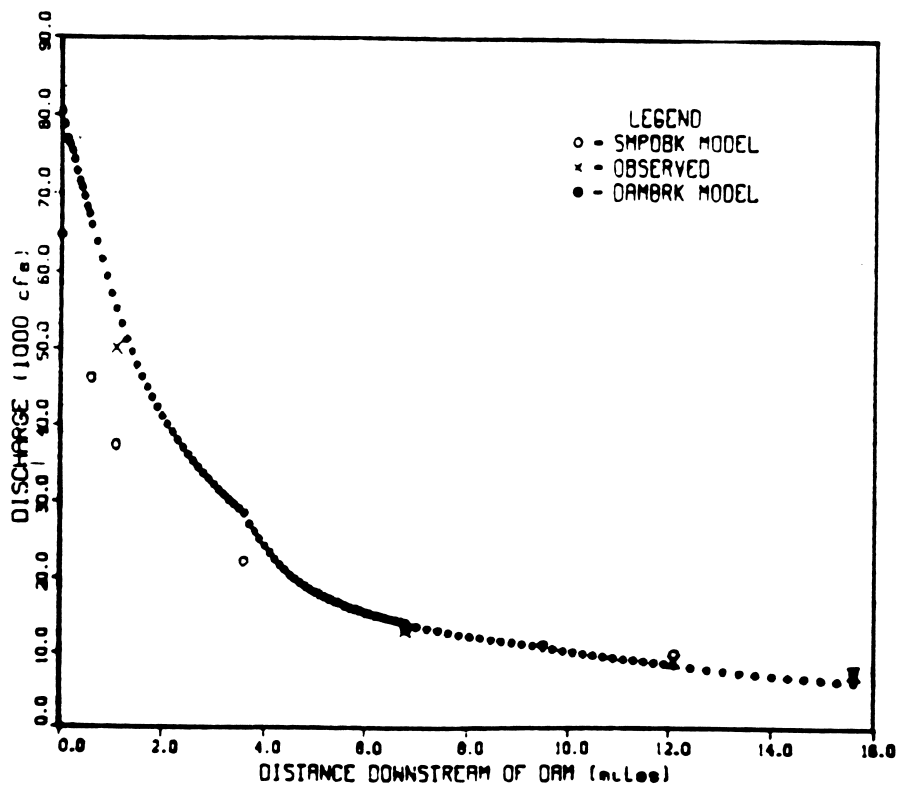


FIG. 2 PROFILE OF PEAK DISCHARGE DOWNSTREAM OF BUFFALO CREEK.

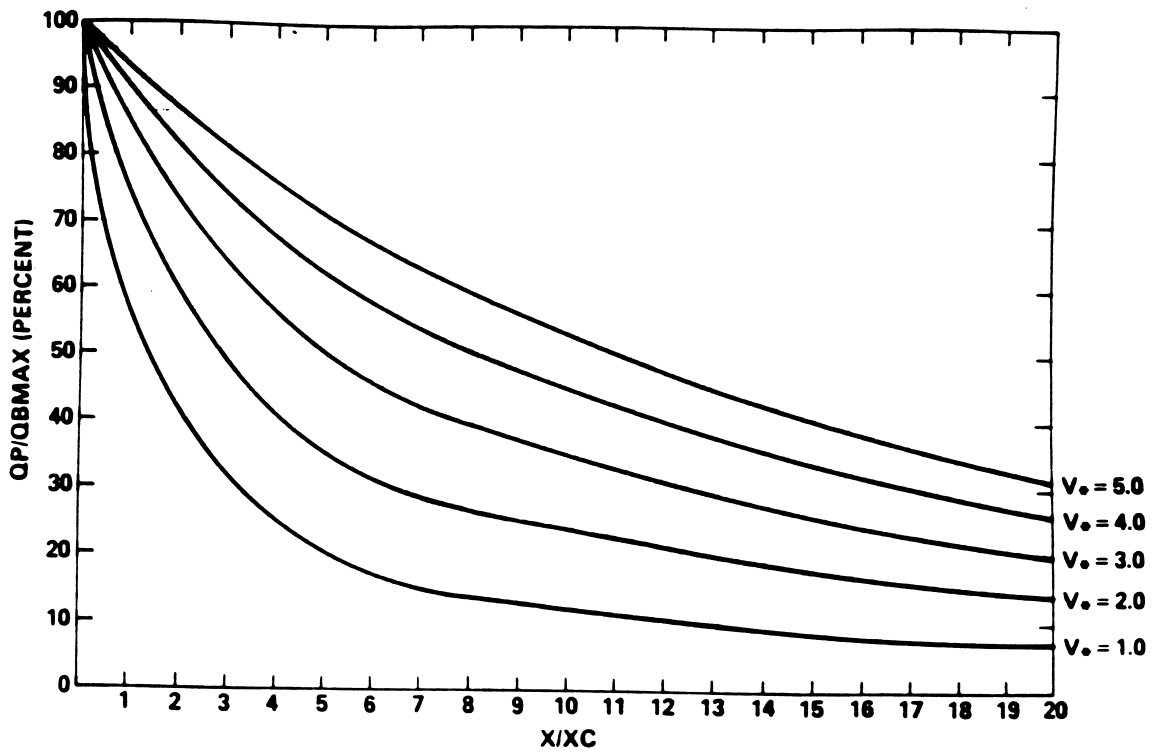


FIG. 3 ROUTING CURVES FOR SMPDBK MODEL FOR FROUDE No = 0.25.

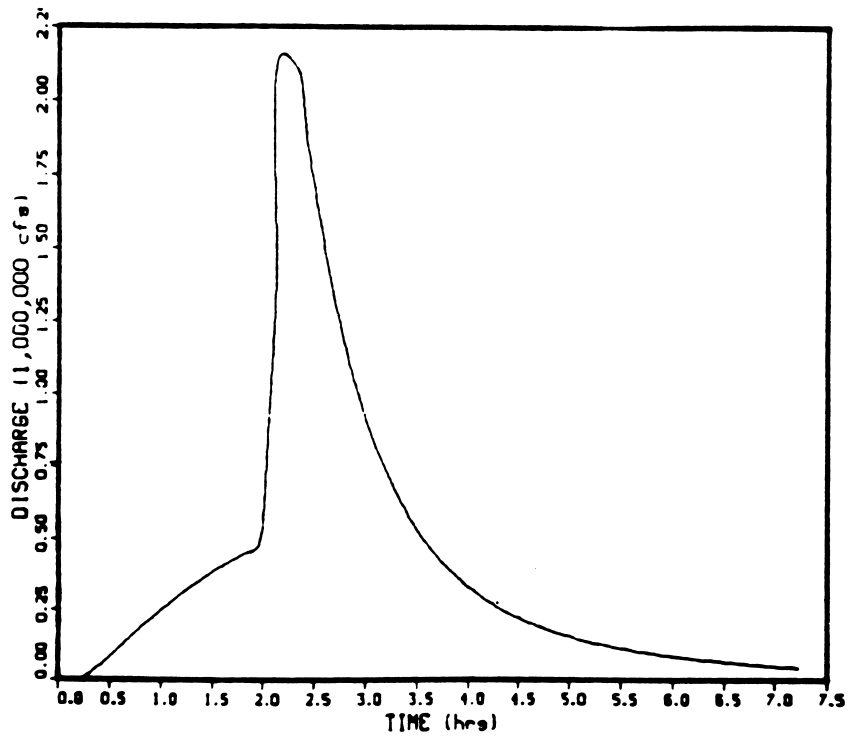


FIG. 4. TETON OUTFLOW HYDROGRAPH PRODUCED BY BREACH MODEL.